Surface chemistry of CVD diamond

I. I. Oleinik, D. G. Pettifor, A. P. Sutton,*1 and J. E. Butler*2
Computational Science Division, Advanced Computing Center, RIKEN

The β-scission growth mechanism at the diamond $(100)(2\times1)$ surface is studied by a combination of nanoscale ab-initio LDA/GGA and semiempirical tight-binding techniques to provide the necessary input into the mesoscale variable time step Kinetic Monte-Carlo (KMC) simulations of CVD diamond growth. The reaction path of the beta-scission reaction is critically examined and the activation barrier of the reverse etching of the methylene adsorbate is deduced. Our quantum mechanical calculations support a previous semiempirical PM3 study confirming that the molecular mechanics values for the entalphy of the reaction are a factor of 2 wrong. This conclusion provides strong support for the preferential etching mechanism introduced into KMC to predict experimentally measured growth rates.

Introduction

Diamond chemical vapor deposition science and technology has developed dramatically over the last decade due to the highly promising and unusual properties of CVD diamond films. The applications are diverse and include hard coatings, tools, optical and electronic components, thermal management, corrosion protection, radiation detection.[1,2] Experimental studies of the growth processes have revealed complex chemistry and physics inside the CVD reactor. In the CVD environment diverse physico-chemical processes take place including activation of reactive species in the gas phase, transport of the reactive species to the growth surface, adsorption, nucleation and subsequent incoporation of the carbon species into the growing diamond film, see Fig. 1. Theoretical and experimental investigations have identified the important growth species, studied the nature and structures of the diamond surfaces, and measured and predicted the growth rates as a function of temperature and reactant fluxes.[3–5]

However, there is still a gap between experiment and theory in the sense that the large experimental database on morphology, crystalline texture, twinning, extended and point defects, and impurity incorporation can not be rationalized consistently within a unified and self-contained theoretical framework. This is primarily due to a lack of understanding of the basic growth mechanisms on diamond surfaces, where, on one hand, the severe chemical environment precludes the monitoring of elementary reaction steps by surface science techniques, and on the other hand, the complexity and size of the system limit the scope and capability for modelling the growth. In principle this gap can be bridged by separating the system into subsystems with different time and length scales and applying appropriate modelling techniques to describe properly the phenomena at the specific level of detail. In the case of CVD diamond growth these hierarchies include the gas phase simulations of the CVD reactor, the mesoscale modelling of the crystal growth and the nanoscale modelling of the surface chemistry during deposition as illustrated in Fig. 1. During the last few years progress has been made in the mesoscale modelling of CVD processes by the kinetic Monte-Carlo (KMC) method.[6–9] Such a lattice-based model, which is fully three-dimensional, enables a detailed study at the atomic level of the structure and morphology of the surface during the growth. An important requirement for the KMC model is that it must simulate crystal growth over macroscopic time scales (seconds to minutes) so that the data on growth rate or film composition may be compared directly to existing experimental results. This requirement of long time scales can be accomplished by the use of the variable time step kinetic Monte Carlo method known as the N-fold Way.[10] This method introduces the temporal evolution into the growth sequence and discriminates between fast and slow reactions by proper increments of the time step.

The variable-time step KMC method has been successfully applied to the modelling of the chemical vapor deposition of diamond thin films.[6–9] Simulations corresponding to hours of growth for surfaces with thousands of atoms per layer were performed on desktop workstations. The calculated growth rates, on both (111)- and (110)-oriented surfaces, were in good agreement with experiment for temperatures ranging from 800 to 1500 K. Furthermore, by simulating the incorporation of point defects, optimum growth temperatures for the production of high-quality films were predicted.

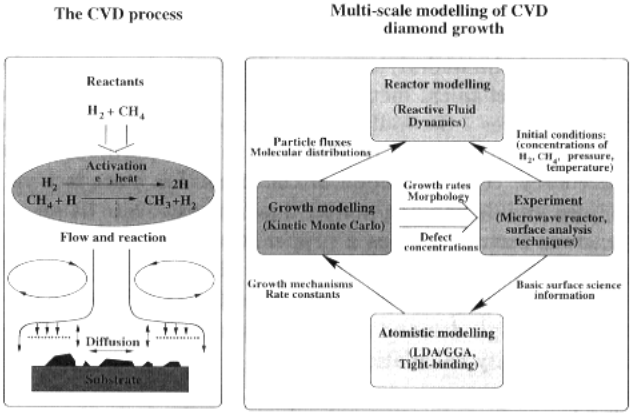

Fig. 1. Schematic of CVD process and multiscale modelling of CVD diamond growth.

*1 Permanent address: Department of Materials, University of Oxford, UK
*2 Permanent address: Gas/Surface Dynamics Section, Naval Research Laboratory, USA

However, the ability of KMC to model realistically three-dimensional deposition processes depends crucially on a detailed understanding of the appropriate growth mechanisms and a reliable database of the rates of the surface chemical reactions. This was clearly demonstrated during the KMC growth modelling of the (100)(2 × 1) diamond surface. Simulations based on the surface kinetics of Harris and Goodwin [11] predict growth on the (100)(2 × 1) surface that is much faster than on the (110) and (111) surfaces in contradiction with experiment. In addition, atomic scale KMC produces atomically rough morphologies in disagreement with scanning probe and other experimental observations.[12–14] Apparently, some steps in the reaction sequence are missing or proceed with different rates. Thus, the nanoscale modeling of the surface chemistry on (100) diamond surface is crucial for reconciling the KMC modelling with experiment.

In this paper we show how quantum-mechanical modelling can aid in building the link between the individual chemical events and the mesoscopic growth model. We particularly focus on the issue of (100) surface growth and consider in detail the β-scission reaction mechanism which feeds into the KMC modelling chain. This will allow the proper kinetics for predicting the experimentally observed growth rates. In section II we outline the general methodology of quantum-mechanical modelling. In section III we consider the kinetics of the β-scission mechanism and its role in the preferential etching of CH_2 groups. This etching mechanism slows down the growth rate on (100) surface by allowing the removal of the undercoordinated carbon atoms and promoting the growth of the smooth regions of the (100)(2 × 1) surface.

Methodology of quantum-mechanical modelling of the surface chemical reactions

To model successfully the chemical reactions that take place on a surface several requirements have to be fulfilled. Firstly, the process of bond making and bond breaking at the surface is accompanied by substantial rearrangements of the atoms around the reactive region. Even for covalently bonded systems, where the bonds are quite localized and the nature of the chemical interaction between the atoms can be modelled via a cluster, the surface relaxation and change in the strain during the course of the reaction have a strong influence on the reaction dynamics. Therefore, in order to take into account the geometrical constraints due to the presence of the surface and the underlying crystal lattice we have to employ quantum-mechanical methods that decribe properly the surface structures. Secondly, the chemical interactions at the transition state have to be modelled at the appropriate level of accuracy. The prediction of the transition state is a very complex and demanding matter due to the delicate balance of numerous factors such as a proper treatment of correlation, spin, size of basis set etc. Obviously, these two requirements of high accuracy yet large simulation cells are difficult to meet due to the high demand on the computer resources required for high quality calculations.

In order to find a compromise between these requirements, we employ a 'multiscale' methodology and divide the system under study into two regions with different length scales. The small area around the reaction zone is treated with high level ab-initio calculations but the large area surrounding this small cluster is treated with low level semi-empirical quantum mechanics but with the proper treament of the solid state environment. Within the small reactive region we employ the local density approximation with the generalized gradient corrections implemented in the code DMol, the MSI software package. Density functional theory has its own limitations and drawbacks especially for transition state calculations. However, the accuracy of 5–10 kcal/mol in barrier heights for hydrocarbon reactions achieved by LDA with gradient corrections[15] is acceptable for our purposes, when the appropriate data base of the gas-phase chemical reactions is available for comparison and guidance. Influence of the size of the basis set, the integration grid and other parameters were carefully studied to ensure the proper quality of the results. In addition, spin was taken into account for the correct description of the process of bond-making and bond-breaking. The size of the cluster is limited by the computational resources available and in our case it is 20–30 atoms.

The large area surrounding the reactive cluster consists of a slab of 5 atomic layers with 16 atoms in each layer. The strength of the carbon-carbon bonds as well as the local nature of the hydrocarbon chemical interactions ensures that the finite size of the slab has negligible influence on the reactive region. The quantum-mechanical forces are calculated within the two-centre, orthogonal tight-binding (TB) model. We use the Xu et al's parametrization for carbon-carbon interactions[16] and Davidson and Pickett[17] and Horsfield et al.[18] paramentrization for C-H interactions. The H-H parameters were fitted to give the proper description of the dissociation of the hydrogen molecule. The tight-binding Hamiltonian is diagonalized at every geometry optimization step and forces are calculated using the Helman-Feynman theorem. An important ingredient of the tight-binding model is the local charge neutrality (LCN) constraint.[19] It is well known from ab-initio calculations that charge redistribution in hydrocarbon systems is quite small with the total charges of atoms close to zero. Therefore, the LCN constraint reflects the proper chemical behaviour of hydrocarbon bonding and also allows us to maintain the homolytic nature of the bond rupture. The tight-binding parametrization of Horsfield et al. has been highly succesful in describing the energetics and geometries of the hydrocarbon molecules and diamond surfaces, so that we would expect a good overall performance of TB in predicting the energetics and bond geometries of stable adsorbate complexes at the diamond surface.

The interface between the tight-binding and LDA/GGA regions is accomplished according to the following scheme. The initial geometric configuration of atoms is determined by the TB structural relaxation of the slab with the constraints imposed on the bottom atoms saturated with hydrogens as well as constraints on the reacting atoms to follow the chosen reaction path. Then the LDA/GGA cluster of fixed size is cut from the TB slab and the C-C bonds that are broken are saturated with hydrogen atoms according to the standard procedure which takes into account the proper change of hybridization of the carbon atom during the structural relaxation. Thus, the shape of the cluster changes during the course of the reaction in order to match the movements of the atoms in the slab. The next step is the structural optimization of the LDA/GGA cluster by DMOL. The consistency with the TB geometry is enforced by keeping all the carbon atoms at the boundaries as well as the 'ghost' hydro-

gen atoms fixed in addition to the constraints imposed on the reacting atoms to follow the chosen reaction path. The constrained geometry optimization is accomplished with the use of the Perdew and Wang (1992) LDA functional.[20] In addition, the energy of the final geometry is calculated using a Becke-Perdew generalized gradient-corrected functional.[20,21] We have tested the difference in geometries optimised by LDA and GGA and found minor differences in the bond lengths and bond angles as was expected. However, the energy differences reflect the well known tendency of LDA to overbinding. The post-GGA corrects this problem of overbinding and gives and error of about 5 kcal for the binding energies of the hydrocarbon molecules and 5–10 kcal/mol for the activation barriers. To make reliable predictions of the transition state we refined the transition state geometry with pure GGA forces.

A very important question has to be answered: how consistent is the TB geometry with the geometry obtained by LDA? The answer is that the structures obtained by TB and LDA are almost the same except in the region in the vicinity of the transition state. It takes one to two geometry optimization steps to refine the minimum energy structure starting from the TB geometry. The substantial difference in the vicinity of the transition state can be explained by the deficiency of the TB parametrization to treat the long range C-C interactions that are not screened by the presence of other atoms. At the transition state the distance between the adsorbed methylene carbon and the carbon atom at the other end of the dimer bond is around 2.2 Å. This is very close to the TB cut-off so that the TB predicts zero interaction between these atoms. This is in contrast to the small but nonzero C-C interaction which can be seen in the DMol simulations from the change of the sp^2 hybridization of the methylene carbon to an intermediate hybridization which distorts the planar geometry of the methylene. Therefore, it is very important for predicting transition state structure to refine the cluster geometry by an LDA rather than a TB calculation.

Quantum mechanical modelling of the β-scission growth mechanism at the diamond (100) surface

The chemical vapor deposition of diamond proceeds through the adsorption and subsequent incorporation of various hydrocarbon fragments at the diamond surface. The characteristic feature of the CVD environment is the presence of a high flux of atomic hydrogen 10^{19}–10^{21} $cm^{-2}sec^{-1}$ which is created by the plasma, hot fialment or combustion flame. As a result of the rich abundance of hydrogen the diamond surface is fully hydrogenated although dangling bond radical vacancies appear from time to time as a result of atomic hydrogen abstraction. Several reaction mechanisms have been proposed to account for growth on the (100) 2×1 reconstructed surface. The most plausible one was proposed by Brenner, Garrison and collaborators based on the addition of a methyl radical and the subsequent insertion of a CH_2 group into the dimer bond following the hydrogen abstraction,[22] see Fig. 2. (The reaction pathway for growth from methyl radicals at (100) surface). The most important reaction step in this sequence is the so called beta-scission reaction when the carbon in the methylene group forms a double bond with the dimer carbon atom and the dimer bond is broken as a result of the formation of this double bond. The insertion of the CH_2 group into the opened dimer is the key step for adsorbate incorporation into the diamond lattice.

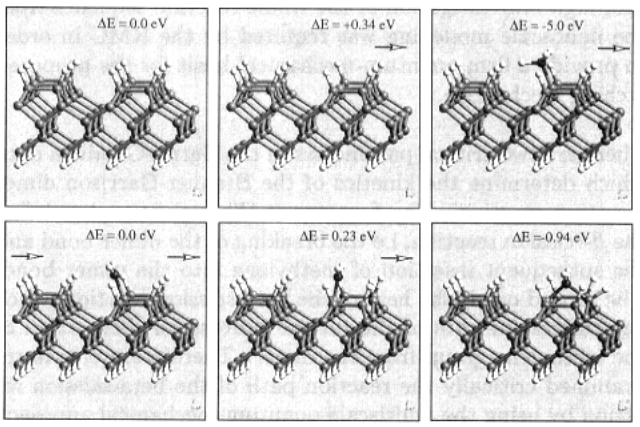

Fig. 2. Growth mechanism on diamond (100)(2 × 1) surface.

The variable step kinetic Monte-Carlo simulations of diamond (100) growth based on the Harris-Goodwin reaction kinetics faced several difficulties in reproducing the well-known experimental observations. Firstly, the growth rate at (100) is too fast compared to the growth at the (110) and (111) faces. The diamond growth on (100), (110) and (111) faces requires the incorporation of one, two and three carbon atoms respectively. The KMC growth rate would reflect this trivial mechanistic rule giving the (100) face as the fastest and the (111) as the slowest growing faces. Obviously, this discrepancy between experiment and KMC kinetics questions the rates of the reactions in the Harris-Goodwin table or indicates the presence of other reactions which were not considered previously. The preferential etching mechanism was introduced in order to slow down the growth rate on the (100) surface. It was assumed in the KMC modelling that the Brenner-Garrison reaction of methylene insertion into the dimer bond is totally irreversible. However, the reverse sequence can make possible the de-insertion of the methylene and the subsequent abstraction of this group by atomic hydrogen. A two step etching rate can be deduced from the Harris-Goodwin reaction set by assuming that the rate limiting step of etching is the hydrogen abstraction of the methylene group. Therefore, the fast reactions of insertion and de-insertion are in equilibrium. This gives the rate of etching per carbon site $R_{\rm etch} = A_e \exp(-28.3/RT)$. The activation barrier of 28.3 kcal mol^{-1} comes from the equilibrium constant of reactions (a) and (b) which is determined by the difference in enthalpies of the products and reactants of the direct insertion reaction. The prefactor A_e is equal to $A_e = 10^{14}[H]$, where $[H]$ is the atomic hydrogen concentration. At typical CVD conditions $[H] = 10^{-9}$ mol cm^{-3} and the absolute rate of etching at 1200 K is 0.76 sec^{-1}. The hydrogen abstraction rate at the diamond surface occurs at the rate of 10^7 sec^{-1}, which provides the natural time scale in the system. Compared with this time, the etching rate according to Harris and Goodwin kinetic model is much too slow.

It was thought likely that the molecular mechanics data of Harris and Goodwin are in error. Therefore, the KMC modelling introduced an etching rate to match the experimental data. The KMC "experimetal etching rate" at standard CVD conditions is 2×10^4 sec^{-1} which is several orders of magnitude larger than the Harris/Goodwin number. Obviously, a

thorough reinvestigation of the whole reaction sequence from the nanoscale modelling was required by the KMC in order to provide a firm quantum-mechanical basis for the proposed etching mechanism.

There are two critical parameters in the Harris-Goodwin data which determine the kinetics of the Brenner-Garrison dimer insertion reaction. The first one is the activation barrier of the β-scission reaction, i.e the breaking of the dimer bond and the subsequent insertion of methylene into the dimer bond. The second one is the heat of the beta-scission reaction which determines the rate of the reverse process for deinsertion of the methylene group from the dimer. Therefore, we have re-examined critically the reaction path of the beta-scission reaction by using the multiscale quantum-mechanical approach outlined in the preceding section. This particular surface reaction has a single natural reaction coordinate, that is the coordinate of the methylene carbon along the direction of the dimer bond. Therefore, we implemented a simple scheme for the one-dimensional search for the transition state. We constrained the carbon atom to be in the plane perpendicular to the reaction coordinate. All the other atoms in the reactive region were allowed to move and the system was optimized to get the energy minimum at every point along the reaction coordinate.

The potential energy profile along the reaction coordinate is shown in Fig. 3 with the appropriate structures of the reactants, products and transition state. The activation barrier E_a and the heat of the beta-scission reaction H are 13.6 kcal mol^{-1} and 12.3 kcal mol^{-1}. These numbers should be compared with the Harris-Goodwin data E_a = 8.8 kcal mol^{-1} and H = 28.3 kcal mol^{-1}. The Harris-Goodwin activation barrier is quite close to our barrier and the reason is quite simple. This number has been obtained in the work of[23] by employing high quality CI tehniques. However, the heat of the reaction has been obtained with the use of molecular mechanics. Therefore, the 100% error is not surprising. The deficiency of the MM3 force field in this particular situation is explained by the application of the method beyond the region of its validity. Interestingly, the activation barrier and the heat of the reaction are in good agreement with PM3 calculations by S. Skokov et al.,[24] that is E_a = 15.3 kcal mol^{-1} and H = 14.6 kcal mol^{-1}.

What are the implications of the results for KMC modelling? Firstly, we predict the activation barrier for the etching rate to be two times smaller than the Harris-Goodwin barrier. Our absolute value of the etching rate is in a good agreement with the KMC "experimental" value (6×10^4 sec^{-1} compared to 2×10^4 sec^{-1} respectively). Thus, our calculations support the preferential etching mechanism which was suggested by KMC. Secondly, the difference in the activation energies will result in a different temperature dependence for the net etching rate. A deviation of the KMC growth rate from experimental data has been observed during the KMC runs, so that this issue has to be reexamined more thoroughly with the use of the newly derived etching rates.

Another interesting aspect of preferential etching is that it can explain the growth of the atomically smooth 2×1 dimer reconstructed areas. The ordering would be present of the atomic hydrogen can etch the isolated methylene groups inserted into dimer, thus disallowing the island growth mode.

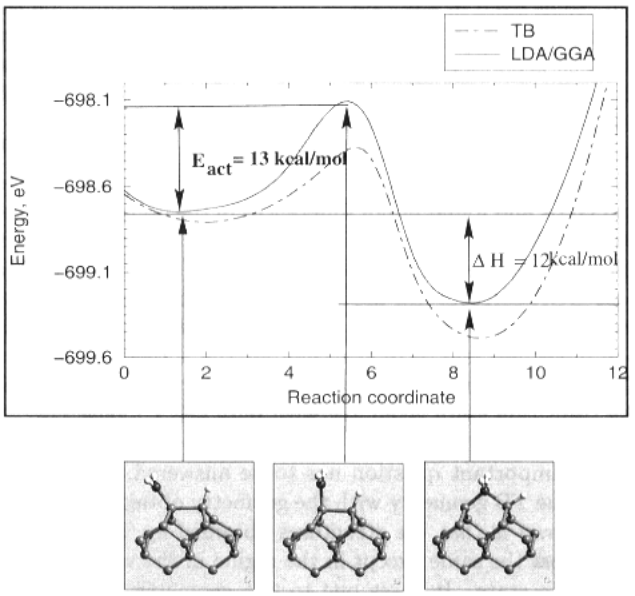

Fig. 3. Reaction path of the β-scission reaction.

The formation of ordered domains would then be possible if the etching of already assembled etching groups were highly prohibited from the thermodynamical point of view. For this purpose we calculated the heat of removal of the CH_2 group from the middle of the three bridge methylene complex and from the side of the three bridge complex. We have obtained the following energies for the etching reactions: from the middle—100.8 kcal mol^{-1}, from the side—39.4 kcal mol^{-1}. These numbers can be compared with the heat of etching of the isolated CH_2 unit—15.68 kcal mol^{-1}. Two conclusions can be drawn from these results: (i) the etching of the isolated CH_2 unit is much more feasible as compared to etching from an already assembled domain (ii) etching from the side end of the domain is thermodynamically more preferable as compared to etching from the middle of the island, thus disallowing the formation of voids.

Conclusions

We have considered the β-scission mechanism of the diamond (100) growth and have demonstrated that the quantum-mechanical modelling has been successful in predicting the key parameters governing the kinetics at the atomic scale. Feeding the information into the KMC variable time step kinetic Monte Carlo model we have achieved agreement with the experimentally measured growth rates. This demonstrates the importance of linking together different modelling hierarchies for realistic modelling of the CVD growth of diamond films. The overall success of this approach encourages us to apply this methodology to other areas of vapour phase processing.

We gratefully acknowledge the Advanced Computing Center of the Institute of Physical and Chemical Research for providing computer time at the Fujitsu VPP500 and VPP700 supercomputers.

References

1) Diamond Films: *Recent Developments*, ed. D. M Gruen and I. Buckley-Golder, MRS Bulletin **23**, 9 (1998).
2) *Handbook of Industrial Diamonds and Diamond Films*: ed. M. A. Prelas, G. Popovici, and L. K. Bigelow, (Mracel Dekker, New York, 1998), p. 527.
3) D. G. Goodwin and J. E. Butler: *Handbook of Industrial Diamonds and Diamond Films*, ed. M. A. Prelas, G. Popovici, and L. K. Bigelow, (Mracel Dekker, New York, 1998).
4) M. P. D'Evelyn: in *Handbook of Industrial Diamonds and Diamond Films*, ed. M. A. Prelas, G. Popovici, and L. K. Bigelow, (Mracel Dekker, New York, 1998), p. 89.
5) M. Frenklach and S. Skokov: J. Phys. Chem. B **101**, 3025 (1997).
6) C. C. Battaile: Ph. D. thesis, University of Michigan (1998).
7) C. C. Battaile, D. J. Srolovitz, and J. E. Butler: J. Appl. Phys. **82**, 6293 (1997).
8) D. J. Srolovitz, D. S. Dandy, J. E. Butler, C. C. Battaile, and Paritosh: JOM **49**, 42 (1997).
9) M. Frenklach: J. Chem. Phys. **97**, 5794 (1992).
10) A. B. Bortz, M. H. Kalos, and J. L. Ledowitz: J. Comp. Phys. **17**, 10 (1975).
11) S. J. Harris and D. G. Goodwin: J. Phys. Chem. **97**, 23 (1993).
12) Y. Kuang, Y. Wang, N. Lee, A. Badzian, T. Badzian, and T. T. Tsong: Appl. Phys. Lett. **67**, 3721 (1995).
13) B. D. Thoms and J. E. Butler: Surf. Sci. **328**, 291 (1995).
14) H. Sasaki, M. Aoki, and H. Kawarada: Diam. Relat. Mater. **2**, 1271 (1993).
15) A. C. Scheiner, J. Baker, and J. W. Andzelm: J. Comput. Chem. **18**, 775 (1997).
16) C. H. Xu, C. Z. Wang, C. T. Chan, and K. M. Ho: J. Phys. Condens. Matter **4**, 6047 (1992).
17) B. N. Davidson and W. E. Pickett, Phys. Rev. B **49**, 11253 (1994).
18) A. P. Horsfield, P. D. Goodwin, D. G. Pettifor, and A. P. Sutton: Phys. Rev. B **54**, 15773 (1996).
19) A. P. Sutton, M. W. Finnis, D. G. Pettifor, and Y. Ohta: J. Phys. C **21**, 35 (1988).
20) J. P. Perdew and Y. Wang: Phys. Rev. B **45**, 13244 (1992).
21) A. D. Becke: J. Chem. Phys. **88**, 2547 (1988).
22) B. J Garrison, E. J. Dawnkaski, D. Strivastava, and D. W. Brenner: Science **225**, 835 (1992).
23) C. B. Musgrave, S. J. Harris, and W. A. Goddard: Chem. Phys. Lett. **247**, 359 (1995).
24) S. Skokov, B. Weiner, and M. Frenklach: J. Phys. Chem. **98**, 8 (1994).